KdV Solitons and Solitary Water Wave Collisions

Elliot Jarmain
University of Toronto
4^{th} Year Research Project
Supervising Professor: Stephen Morris
(Dated: April 5, 2019)

Solitary waves were produced in a narrow channel-shaped tank filled with water. Images of the waves were taken at 100 frames per second as the wave propagated. Image analysis methods were used to convert the images into position data for the water's surface. This data was then compared to the Korteweg-deVries (KdV) equation to determine if the waves being produced were KdV solitons. Counter-propagating soliton collision were studied, as were collisions between one soliton and the end of the tank. These were compared with the theoretical predictions of Su & Mirie [10] and the experimental data of Maxworthy [9].

I. INTRODUCTION

Solitary waves are localized nonlinear waves that propagate at a constant velocity and maintain their shape as they travel. They occur in nature due to a balance between the non-linear properties of the medium and dispersion, and can be modelled by an exact solution to the Korteweg-deVries (KdV) equation. Solitary waves retain their initial velocity and shape after a collision with another solitary wave, and are consequently referred to as "solitons".

During head-on collisions, the maximum run-up amplitude of the solitons is greater than the superposition of the incident waves. After collisions, the trajectories of the solitons experience a phase lag from the incident trajectories. These phenomena have been studied experimentally in [9], theoretically in [10], and numerically in [5].

The goal of this experiment is to determine whether the solitary waves produced by our apparatus are indeed KdV solitons, and to determine if the characteristic properties of run-up and phase-lag are observed during collisions between two solitary waves and during collisions with one solitary wave with the end wall.

II. THEORY

A solitary water wave propagating in the $+x$ direction can be modelled by an exact solution to the KdV equation [2].

In the laboratory frame, the KdV equation in physical units is as follows:

$$\left(\frac{1}{c_0}\right) h_t + h_x + \left(\frac{3}{2H}\right) h h_x + \left(\frac{H^2}{6}\right) h_{xxx} = 0 \qquad (1)$$

where H is the quiescent water depth, $h(x,t)$ is the elevation above the quiescent depth as a function of position x and time t, and $c_0 = \sqrt{gH}$ where g is gravitational acceleration.

The exact solution to (1) is found to be

$$h(x,t) = h_0 \operatorname{sech}^2\left[\frac{1}{2H}\sqrt{\frac{3h_0}{H}}\left(x - c_0\left[1+\frac{h_0}{2H}\right]t\right)\right] \qquad (2)$$

$$= h_0 \operatorname{sech}^2\left[\frac{x-Ut}{w}\right], \qquad (3)$$

where h_0 is the wave's amplitude (see FIG. 1.), and the speed U and width w are given by

$$U = c_0\left[1+\frac{h_0}{2H}\right], \qquad w = 2H\sqrt{\frac{H}{3h_0}}\,. \qquad (4)$$

Note that the only free parameter in (2) is h_0.

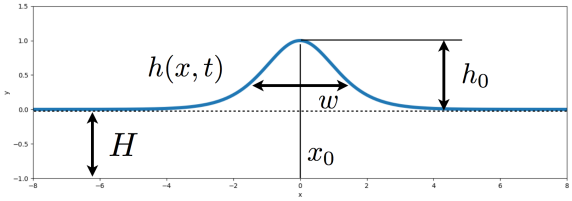

FIG. 1: A visual showing the parameters in equations (2) and (3). Source: [1]

A. Collisions

1. Run-up

The maximum amplitude of two colliding solitary waves is greater than the sum of the amplitudes of the incident waves. Su & Mirie [10] found through perturbation analysis, to third order, that the maximum amplitude reached during collision is given by

$$\varepsilon_{max} = \varepsilon_R + \varepsilon_L + \frac{\varepsilon_R\varepsilon_L}{2} + \frac{3}{8}\varepsilon_R\varepsilon_L(\varepsilon_R + \varepsilon_L) \qquad (5)$$

where $\varepsilon = h_0/H$ is the dimensionless amplitude. The subscripts R and L refer to the right and left waves respectively and ε_{max} is the dimensionless amplitude during the peak of the collision.

2. Phase-lag

Solitary waves exhibit a retardation in phase after a head-on collision. Su & Mirie [10] show that the phase lag after collisions is given by

$$\Delta\theta_R = H\left(\frac{\varepsilon_L}{3}\right)^{1/2}\left(1+\frac{\varepsilon_L}{8}+\frac{3\varepsilon_R}{4}\right) \tag{6}$$

$$\Delta\theta_L = -H\left(\frac{\varepsilon_R}{3}\right)^{1/2}\left(1+\frac{\varepsilon_R}{8}+\frac{3\varepsilon_L}{4}\right). \tag{7}$$

However, Maxworthy (see Figure 3 from [9]) showed experimentally that the phase lag and the amplitude of the incident waves have no correlation.

III. APPARATUS

The experiments described here were performed in a channel-shaped tank filled with water. At one end of the tank is the wavemaker, a motor powered paddle that generates the solitary waves. At the other end is a wall, off of which the solitons reflect. Images of the solitons as they propagate down the wave tank are captured by a 120 fps camera. The water is coloured with red dye and backlit by a 60 V LED light to aid in the surface detection process. The region in which data for the propagating solitons could be collected is just over one metre long. The quiescent water depth can be set up to 10 cm without risk of the water leaving the tank when solitary waves are produced.

IV. METHOD

The images of the waves were cropped so as to remove everything except the water and the backlit region (FIG. 2). The images were then analyzed pixel by pixel to determine which pixels were red and which were not, yielding binary data. The vertical pixel columns were then scanned to determine where the red pixels met the not red pixels, thus determining the location of the water's surface. A visualization of this data is shown in FIG. 3. Two sources of systematic error that arise from this method of data acquisition are parallax and wave shadows. The error that arises from parallax is practically negligible, as can be seen by viewing an image of a metre stick. However, when a wave propagates down the tank it leaves a trailing residue on the front facing wall of the tank (as can be seen in FIG. 2). Sometimes it is possible to set the colour thresholds so not to include this "shadow" in the edge data but other times it is not.

FIG. 2: Cropped image of solitary wave propagating down the tank

FIG. 3: Visualization of the edge data describing the location of the water's surface obtained from FIG. 2

V. ANALYSIS

A. KdV Equation

Sets of images for solitons of various sizes with various quiescent water depths were converted to edge data using the methods described in Sec. IV. The time interval between each pair of images was set to 0.01 seconds. Each frame of a given set was fit to the exact solution of the KdV equation (2). An example of such a fit is shown in FIG. 4. The data was converted from pixel data to physical units using a calibration image of a metre stick. The systematic error that arises from this calibration is small in comparison to other sources of systematic error, namely the difference between the data and the KdV solution.

From these fits, values for the amplitude h_0, position x_0, and width w were extrapolated from the fit parameters. A plot of the position x_0 in relation to time was fit linearly to determine the wave-speed U. All of the data was then normalized so that properties of solitons propagating along water of different quiescent depths could be compared. Distance measurements (x_0, h_0, and w) were normalized by H, speed U was normalized by $c_0 = \sqrt{gH}$, and time was normalized by $\sqrt{H/g}$.

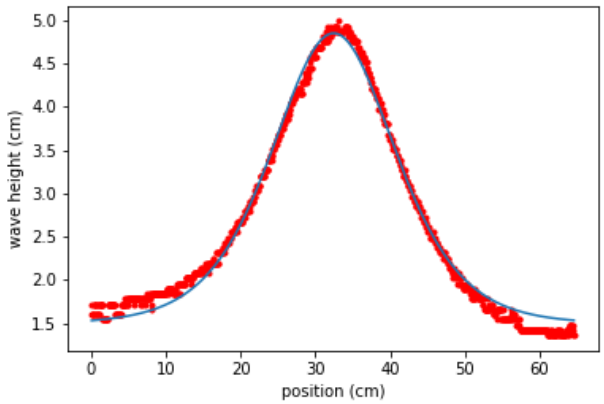

FIG. 4: The data from FIG. 3. fit to the solution to the KdV Equation (2)

A plot of various dimensionless speeds in relation to the dimensionless amplitude of the wave is shown in FIG. 5. The green line shows the relationship between speed and amplitude given by (4). A plot of various dimensionless widths in relation to the dimensionless amplitude of the wave is shown in FIG. 6. The green line again shows the relationship between width and amplitude given by (4).

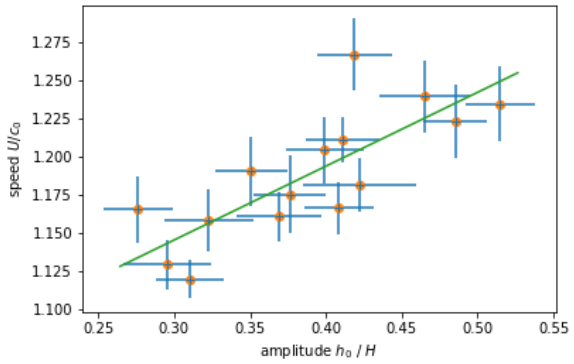

FIG. 5: Dimensionless speed plotted against dimensionless amplitude. The green line shows the relationship predicted by (4)

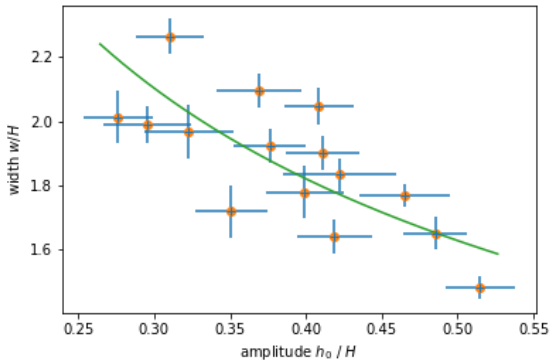

FIG. 6: Dimensionless width plotted against dimensionless amplitude. The green line shows the relationship predicted by (4)

Nine of the fifteen data points for dimensionless speed plotted against dimensionless amplitude in FIG. 5 agree with equation (4) within error, while only five of fifteen points agree for dimensionless width plotted against dimensionless amplitude in FIG. 6. The poor quality of the fit for the width data could be due in part to the effects of the wave "shadow" described in Sec. IV.

B. Head-on Collisions

Head-on collisions were produced by sending a solitary wave down the tank to reflect off the end wall, then sending a second solitary wave to collide with the first, as shown in the space-time plot (FIG. 7.).

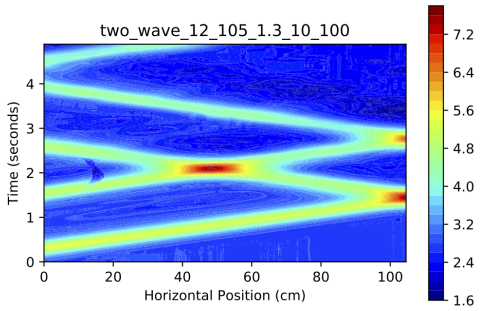

FIG. 7: Space-time plot of two waves colliding head-on

1. *Phase lag*

Before and after the two waves collided, their positions x_0 and amplitudes h_0 were calculated using the methods described in Sec. V A. The trajectories of the two waves could then be plotted in the regions before and after the collision and the wave-speed and phase lag could be determined. An example of such a plot is shown in FIG. 8, where the wave coming from the right has dimensionless amplitude $\varepsilon_R = 0.27 \pm 0.02$, the left wave has dimensionless amplitude $\varepsilon_L = 0.29 \pm 0.02$, and the quiescent water depth is $H = 7.2 \pm 0.1$ cm. The measured phase lags for the two waves shown in FIG. 8 are $\Delta\theta_R = 11.9 \pm 2.6$ and $\Delta\theta_L = -11.7 \pm 1.4$ cm. The values for $\Delta\theta_R$ and $\Delta\theta_L$ that we obtain by plugging $\varepsilon_R = 0.27 \pm 0.02$ and $\varepsilon_L = 0.29 \pm 0.02$ into equations (6) and (7) are 2.77±0.06 cm and -2.70±0.06 cm respectively. These are significantly smaller than the experimental values for $\Delta\theta_R$ and $\Delta\theta_L$. Note, however, that the wave with the smaller amplitude experiences a greater phase lag, as predicted by equations (6) and (7). Also note, that the experimental results of Maxworthy [9] do not obey the theoretical predictions of Su & Mirie [10] given by equations (6) and (7). A look at Figure 3 from [9] shows that regardless of the amplitude of the incident waves, the phase lag is just over $1.2 \times H$ (Maxworthy's experiments were done only with two waves of equal amplitudes). Considering that our incident amplitudes were almost equal and our equilibrium depth was set at $H = 7.2 \pm 0.1$ cm, taking $1.2 \times H$ yields $\Delta\theta = 8.6$ cm, which is still less than the phase lag values we obtained, but much closer. It is also worth considering that equations (6) and (7) desribe the phase lag long after the collision has occurred. From [5] and [11], we know that the phase lag is greater right after the collision than long after the collision. It is possible that our wave tank is not long enough to measure the phase lag far away enough from the collision to agree with (6) and (7). Another cause for discrepancies between our measured phase lag and equations (6) and (7) could be that the right wave is still experiencing effects of its collision with the end of the tank.

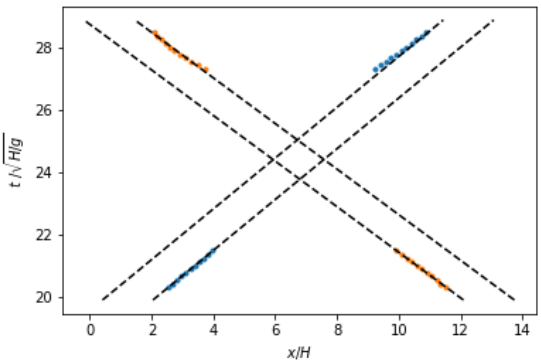

FIG. 8: ε_L (blue)$= 0.29 \pm 0.02$, ε_R (orange)$= 0.27 \pm 0.02$

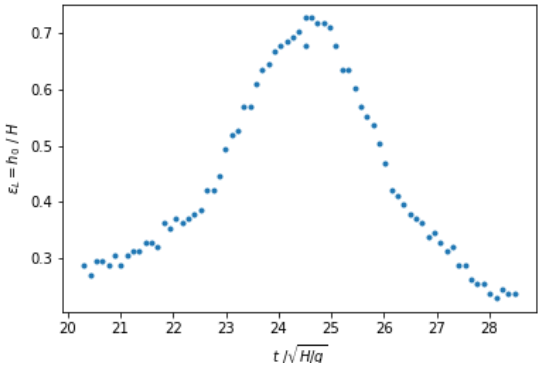

(a) The dimensionless amplitude $\varepsilon_L = 0.29 \pm 0.02$ before, during, and after the collision

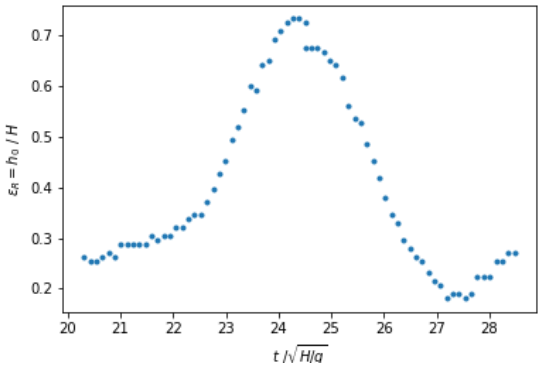

(b) The dimensionless amplitude $\varepsilon_R = 0.27 \pm 0.02$ before, during, and after the collision

FIG. 9

2. *Run-up*

Since the frames and corresponding edge data during the collision are not modelled by equation (2), the amplitude during the collision had to be determined by simply taking the maximum height value in the data for the water's surface (as opposed to taking the h_0 term of the fit to (2)). The maximum run-up data for the $\varepsilon_R = 0.29 \pm 0.01$ and $\varepsilon_R = 0.27 \pm 0.01$ waves from Sec. V B 1 are shown in FIG. 9. Notice how in FIG. 9b, after the collision the amplitude dips below its incident amplitude then returns to the incident amplitude. According to [5], this phenomenon occurs in the numerical solution of two colliding solitons. More specifically, the amplitude is supposed to dip below the incident amplitude then return to the incident amplitude asymptotically (see Figure 4 from [5]), however our wave tank is too small and our amplitude measurements are too imprecise to witness any asymptotic behaviour. In FIG. 9a, the image region is too small to detect the amplitude returning to its incident amplitude after the collision.

Since we are considering the same collision as in Sec. V B 1, again we have that $\varepsilon_R = 0.27 \pm 0.02$ and $\varepsilon_L = 0.29 \pm 0.02$. The measured run-up ε_{max} obtained by analyzing the edge data of the collision is $\varepsilon_{max} = 0.73 \pm 0.02$. The value obtained for maximum run-up by plugging $\varepsilon_R = 0.27 \pm 0.02$ and $\varepsilon_L = 0.29 \pm 0.02$ into equation (5) is 0.62 ± 0.04. Our experimental measurement for run-up exceeds the theoretical prediction for run-up from [10], albeit not as much as our measurement for phase-lag exceeded the theoretical prediction. However, if we again compare our experimental result to Maxworthy (see Figure 4 from [9]) we find that our results our in agreement: two waves colliding, each with dimensionless amplitude slightly less than 0.3, should produce a maximum run-up between 0.7 and 0.8.

3. *Collisions with the end of the tank*

Reflections with the end of the tank were analyzed using methods similar to the analysis done on head-on collisions. When a solitary wave collides with the end of the wave tank, this can be interpreted as the wave undergoing a head-on collision with its reflection. Setting $\varepsilon_R = \varepsilon_L \equiv \varepsilon$ in equation (5) yields

$$\varepsilon_{max} = 2\varepsilon + \frac{\varepsilon^2}{2} + \frac{3}{4}\varepsilon^3. \tag{8}$$

Setting $\varepsilon_R = \varepsilon_L \equiv \varepsilon$ in equation (6) yields

$$\Delta\theta = H\left(\frac{\varepsilon}{3}\right)^{1/2}\left(1 + \frac{7\varepsilon}{8}\right) \tag{9}$$

FIG. 10 and FIG. 11 show the run-up and phase-lag of a solitary wave with initial amplitude $\varepsilon = 0.54 \pm 0.01$ colliding with the end wall. The water depth is 6.6 ± 0.1 cm.

The maximum run-up amplitude is measured (from the data shown in FIG. 10) to be 8.4 ± 0.1 cm,
i.e. $\varepsilon_{max} = 1.27 \pm 0.03$. Plugging $\varepsilon = 0.54 \pm 0.01$ into equation (8) yields $\varepsilon_{max} = 1.34 \pm 0.05$. These values agree within error. It is interesting to note that while our data for head-on collisions between two waves did not agree with the theoretical prediction for run-up, our data for

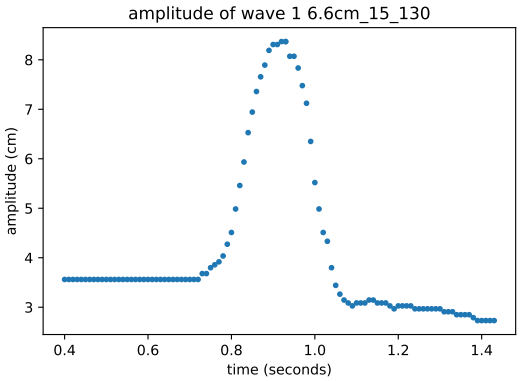

FIG. 10: The dimensionless amplitude $\varepsilon = 0.54 \pm 0.01$ before, during, and after colliding with the end of the tank

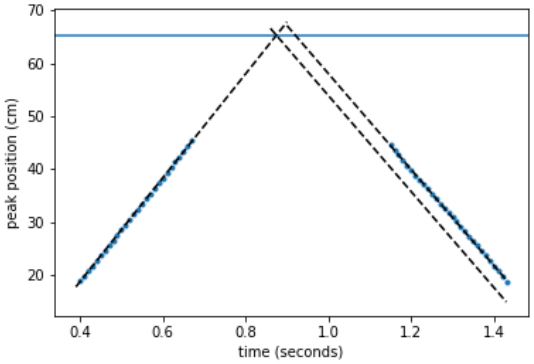

FIG. 11: Trajectory of an $\varepsilon = 0.54 \pm 0.01$ wave reflecting off the end of the tank. The blue dots are data, the solid horizontal line is the position of the wall, and the dashed lines show the trajectories of the data as well as the trajectory of an elastic collision off of the wall. The water depth H is 6.6±0.1 cm.

reflections off the end of the tank did agree. This also occurs with Maxworthy's experimental data, as can be seen in Figure 4 of [9]. Note how the amplitude after the collision is less than the incident amplitude (FIG. 10). Again, unfortunately the region in which data can be collected is too small to observe if the amplitude asymptotically returns to its initial value. It is possible that since this wave is interacting with the end wall, the dissipative effects of the collision mean that the amplitude after the collision will remain at this lower value.

The phase lag of FIG. 11 is measured to be 4.2±0.1 cm. Plugging $\varepsilon = 0.54 \pm 0.01$ into equation (9) gives us $\Delta\theta = 4.1 \pm 0.1$ cm. These values also agree. Note that there is an additional source of systematic error stemming from the measurement of the position of the end wall. The wall's location was determined by inspecting the uncropped images. The error in its location in the image is 2 pixels which corresponds to about 0.1 cm. A change in the position of the end wall directly corresponds to a change in the phase lag measurement, so if the wall's position was actually 0.1 cm to the left, the phase lag would be 0.1 cm larger. Hence, the measurement of the phase lag is actually 4.2±0.1±0.1 cm.

VI. SUMMARY & CONCLUSIONS

Solitary waves were produced in a narrow channel filled with water. The position of the surface of the water as the wave propagated down the channel was determined using image analysis. The speed, width, and amplitude data collected for waves of various sizes at various quiescent water depths were compared with the relationships predicted by the exact solution to the KdV equation. It was found that the speed obeyed the KdV equation to a reasonable extent. And although the width decreased as amplitude increased, it did not fit the relationship predicted by the KdV equation. This could be due to the KdV equation not being an adequate model for the waves produced in this experiment, or due to systematic errors that arise when converting the images into edge data of the water.

Collisions between solitons were then studied, first between two seperate solitary waves then between a single solitary wave and its reflection when it collides with the end wall of the wave tank. Although the two solitons colliding head-on qualitatively exhibited the phase shift and run-up properties expected of colliding solitons, the measurements of these phenomena did not agree with the theoretical predictions (equations (5), (6), & (7)) of Su & Mirie [10]. However, neither did Maxworthy's experimental data [9], with which our run-up measurement agrees. It is possible that the region in which wave data is collected is too small to properly witness properties of the two incident waves far away enough from the collision.

The run-up and phase lag of a single soliton colliding with the end of the tank did agree with the predictions of [10]. Maxworthy's experimental data for collisions with the end wall agreed with the theoretical predictions also. However, more recent experiments on head-on solitary wave collisions, such as [5] and [12] have gotten the experimental data and theoretical predictions of two colliding waves to agree as well.

[1] S. Morris, *Solitons*, Advanced Physics Laboratory Manual (2018).

[2] T. Dauxois and M. Peyrard, *Physics of Solitons*, Cambridge University Press (2006).

[3] R. S. Johnson, *A Modern Introduction to the Mathematical Theory of Water Waves*, Cambridge University Press (2010).

[4] D. J. Acheson, *Elementary Fluid Dynamics*, Oxford University Press (1990).

[5] W. Craig, P. Guyenne, J. Hammack, D. Henderson, and C. Sulem, *Solitary water wave interactions*, *Phys. Fluids*, **18**, 057106 (2006).

[6] C. S. Gardner, J. M. Greene, M. D. Kruskal, R. M. Miura, *Method for Solving the Korteweg-deVries Equation*, *Phys. Rev. Lett.*, **19**, 1095 (1967).

[7] H. Borluka and H. Kalischb, *Particle dynamics in the KdV approximation*, Wave Motion, **49**, 691 (2012).

[8] J. G. B. Byatt-Smith, *An integral equation for unsteady surface waves and a comment on the Boussinesq equation* , *J. Fluid Mech.*, **49**, 625 (1971).

[9] T. Maxworthy, *Experiments on collisions between solitary waves*, *J. Fluid Mech.*, **76**, 177 (1976).

[10] C. H. Su and R. M. Mirie, *On head-on collisions between two solitary waves*, *J. Fluid Mech.*, **98**, 509 (1980).

[11] J. D. Fenton and M. M. Rienecker, *A Fourier method for solving nonlinear water-wave problems : application to solitary-wave interactions*, *J. Fluid Mech.*, **118**, 411 (1982).

[12] Y. Chen and H. Yeh, *Laboratory experiments on counter-propagating collisions of solitary waves. Part 1. Wave interactions*, *J. Fluid Mech.*, **749**, 577 (2014).